Research Article

Yuan Du, Haichao Li, Qingtao Gong*, Fuzhen Pang, and Liping Sun

Dynamic and Sound Radiation Characteristics of Rectangular Thin Plates with General Boundary Conditions

https://doi.org/10.1515/cls-2019-0010
Received Dec 11, 2018; accepted Jan 24, 2019

Abstract: Based on the classical Kirchhoff hypothesis, the dynamic response and sound radiation of rectangular thin plates with general boundary conditions are studied. The transverse displacements of plate are represented by a double Fourier cosine series and three supplementary functions. The potential discontinuity associated with the original governing equation can be transferred to auxiliary series functions. All kinds of boundary conditions can be easily achieved by varying stiffness value of springs on each edge. The natural frequencies and vibration response of the plates are obtained by means of the Rayleigh–Ritz method. Sound radiation characteristics of the plate are derived using Rayleigh integral formula. Current method works well when handling dynamic response and sound radiation of plates with general boundary conditions. The accuracy and reliability of current method are confirmed by comparing with related literature and FEM. The non-dimensional frequency parameters of the rectangular plates with different boundary conditions and aspect ratios are presented in the paper, which may be useful for future researchers. Meanwhile, some interesting points are found when analyzing acoustic radiation characteristics of plates.

Keywords: Dynamic response, Sound radiation, Rectangular thin plate, General boundary conditions

***Corresponding Author: Qingtao Gong:** Ulsan ship and ocean college, Ludong University, Yantai, 264025, PR China; AVIC WEihai Shipyard Co., Ltd, Economic and Techical Develop Zone, Weihai, 264207, PR China; Email: gqt2008@163.com; Tel.: +86-451-82589161
Yuan Du, Haichao Li, Fuzhen Pang, Liping Sun: College of Shipbuilding Engineering, Harbin Engineering University, Harbin, 150001, PR China

1 Introduction

The rectangular plate is one of the most important structures in various engineering branches, such as aerospace, electronics, mechanical, nuclear and marine engineering. A better understanding of its dynamic and acoustic characteristics is meaningful for the designers and engineers. Many studies have been conducted on the vibration and acoustic analysis of plate. Liew *et al.* [1] conducted vibration study on rectangular plates with various combinations of classical boundary conditions by using a orthogonal plate function in the Rayleigh-Ritz procedure. Wu *et al.* [2] analyzed the free-vibration of rectangular thin plates with three classical edge conditions. Different Bessel functions were presented to satisfy the edge conditions such that the governing differential equation and the boundary conditions of the thin plate are exactly satisfied. Mikami *et al.* [3] studied vibration characteristics of rectangular mindlin plates with two opposite edges simply supported by using collocation method. The comparison between collocation method and published results shows the method yields very good results with a relatively small number of collocation points. Liew *et al.* [4] developed the differential quadrature (DQ) method to analyze the free vibration of rectangular plate with generic boundary conditions. Liu *et al.* [5] presented a mesh-free method to analyze the static deflection and the natural frequencies of thin plates with complicated shape. Bert *et al.* [6] proposed two approximate methods namely complementary energy method and differential quadrature method to analyze free vibration of circular and square plates. Wan *et al.* [7] proposed a refined triangular discrete Kirchhoff thin plate bending element RDKT to improve the original element DKT, numerical examples show that present methods indeed improve the accuracy of thin plate vibration analysis. Lim *et al.* [8] proposed a new symplectic elasticity approach for exact free vibration solutions of rectangular Kirchhoff plates based on the conservative energy principle and constructed within a new symplectic space. Li *et al.* [9] employed Green quasifunction method to solve the free vibra-

tion problem of clamped thin plates. Tornabene *et al.* [10–14] studied the dynamic behavior of functionally graded or laminated composite doubly-curved shells and panels of revolution using the Generalized Differential Quadrature (GDQ) method. Kang *et al.* [15] developed a new formulation for the non-dimensional dynamic influence function method, which could extract eigenvalues and mode shapes of clamped plates with arbitrary shapes efficiently. Li *et al.* [16] conducted static and free vibration analysis of laminated composite plates based on nonuniform rational B-splines (NURBS). These researches are mainly focused on free vibration of plates and shells with classical boundary conditions. Thai *et al.* [17, 18] presented an efficient shear deformation theory for vibration of functionally graded plates. Meanwhile, bending, buckling, and vibration analyses of thick rectangular plates with different boundary conditions are also investigated [19, 20]. Two variable refined plate theory is used to investigate free vibration of laminated composite plates by Thai *et al.* [21]. Dozio *et al.* [22] put up an efficient analytical method for quick prediction of the modal characteristics of rectangular ribbed plates. In addition, the Trigonometric Ritz method (TRM) is conducted to analyze general vibration of rectangular orthotropic Kirchhoff plates [23]. Natural frequencies of thin and thick sandwich plates are dealt with using the formulation of advanced two-dimensional Ritz method [24]. Jayasinghe *et al.* [25] presented a Dynamic Coefficient Matrix (DCM) method to investigate the free lateral vibration of a rectangular thin plate, subjected to various boundary conditions. Li *et al.* [26] presented an accurate solution method for the static and vibration analysis of functionally graded Reissner-Mindlin plate with general boundary conditions on the basis of the improved Fourier series method. Shi *et al.* [27] proposed a modeling method to analyze the vibration characteristics of rectangular plates with cutouts having variable size.

Meanwhile, many other studies have been conducted on forced vibration and sound radiation of plates. Allahverdizadeh *et al.* [28] developed a semi-analytical method for forced vibration of a thin functionally graded plate, which proves there is almost no relation between vibration frequencies and amplitudes of plates. Han *et al.* [29] conducted forced vibration of isotropic laminated rectangular plates based on hierarchical finite element method. Akay *et al.* [30] developed an analysis of vibration of clamped plate subjected to transient point force. The sound radiation due to forced vibration of the plate is investigated on the basis of vibration response. Srinivas *et al.* [31] presented a unified exact analysis for the bending, free and forced vibration of simply supported rectangular plates and laminates. Shi *et al.* [32] studied the free and forced vibration characteristics of the moderately thick laminated composite rectangular plates on the elastic Winkler or Pasternak foundations using a new method.

Inalpolat *et al.* [33] studied near field radiation behavior of an unbaffled square plate with free edges, which is excited by a harmonic force at its midpoint. Mace [34] developed a solution for the sound radiation from a point-excited infinite fluid-loaded plate which is reinforced by two sets of parallel stiffeners by using Fourier wavenumber transforms. Laulagnet [35] presented sound radiation of a simply supported unbaffled plate by using a double layer integral representation of the acoustic pressure. Sorokin [36] investigated vibration and sound radiation of sandwich plates with heavy fluid loading. The interaction between acoustic medium and plate is described by boundary integral equations assembled in a two-level system.

The researches mentioned above are mainly focused on free vibration, forced vibration and sound radiation of plates and shells with classical boundary conditions. However, the boundary conditions encountered in practical engineering are always complicated and variable. A unified method which could deal with vibration and acoustic characteristics of rectangular plates subjected to general boundary conditions is necessary and of great significance. Specifically, an improved Fourier series method is now extended to the vibration and sound radiation characteristic of rectangular plates with general boundary conditions.

The transverse displacement of plate is presented by a standard double cosine Fourier series and three supplementary Fourier series. The potential discontinuity of original governing equation is transferred to auxiliary series functions. The change of the boundary conditions can be easily achieved by only varying the stiffness of the boundary springs around the all edges of the plates without involving any change to the solution procedure. The natural frequencies of rectangular plates are obtained by using the Rayleigh–Ritz method. In addition, sound pressure and acoustic radiated power of plates are derived on the basis of displacement response. The reliability and accuracy of current method are adequately validated through a number of numerical examples.

2 Theoretical formulations

2.1 Description of the model

As shown in Figure 1, the length, width and thickness of rectangular thin plate are separately set as a, b and h. The boundary conditions are physically realized in terms

of two kinds of restraining springs (translational and rotational springs) attached to each edge [37–42]. Different boundary conditions can be simulated by changing stiffness of springs. The governing differential equation for vibration of plate under normal load *q(x,y,t)* is as below [43–47]:

$$D\left(\frac{\partial^4 w}{\partial x^4}+2\frac{\partial^4 w}{\partial x^2\partial y^2}+\frac{\partial^4 w}{\partial y^4}\right)+\rho h\frac{\partial^2 w}{\partial t^2}=q(x,y,t) \quad (1)$$

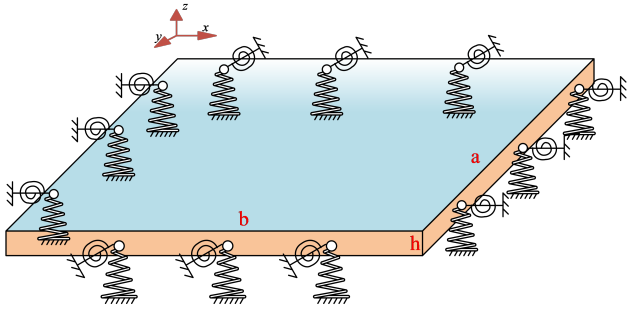

Figure 1: Rectangular thin plate with general boundary condition

When $q(x,y,t)=0$, the governing differential equation is about free vibration of plate and can be simplified as:

$$D\nabla^4 w(x,y)-\rho h\omega^2 w(x,y)=0 \quad (2)$$

Where $\nabla^4=\partial^4/\partial x^4+2\partial^4/\partial x^2\partial y^2+\partial^4/\partial y^4$ is the laplacian operator, $w(x,y)$ is the admissible function of transverse displacement, ω represents circular frequency, $D=Eh^3/(12(1-\mu^2))$ is the flexural rigidity, ρ means the mass density.

According to literature [48–52], the bending moments and the transverse shearing forces in plates can be expressed as below:

$$M_x=-D\left(\frac{\partial^2 w}{\partial x^2}+u\frac{\partial^2 w}{\partial y^2}\right) \quad (3)$$

$$M_y=-D\left(\frac{\partial^2 w}{\partial y^2}+u\frac{\partial^2 w}{\partial x^2}\right) \quad (4)$$

$$Q_x=-D\left(\frac{\partial^3 w}{\partial x^3}+(2-u)\frac{\partial^3 w}{\partial x\partial y^2}\right) \quad (5)$$

$$Q_y=-D\left(\frac{\partial^3 w}{\partial y^3}+(2-u)\frac{\partial^3 w}{\partial y\partial x^2}\right) \quad (6)$$

Rotational and translational springs along each edge correspond to the bending moments and the transverse shearing forces respectively. The boundary conditions for an elastically restrained rectangular plate are as follows:

At $x=0$

$$k_{x0}w=Q_x \quad (7)$$

$$K_{x0}\partial w/\partial x=-M_x \quad (8)$$

At $x=b$

$$k_{xb}w=-Q_x \quad (9)$$

$$K_{xb}\partial w/\partial x=M_x \quad (10)$$

At $y=0$

$$k_{y0}w=Q_y \quad (11)$$

$$K_{y0}\partial w/\partial y=-M_y \quad (12)$$

At $y=a$

$$k_{ya}w=-Q_y \quad (13)$$

$$K_{ya}\partial w/\partial y=M_y \quad (14)$$

Where k_{x0}, k_{xb}, k_{y0} and k_{ya} are respectively translational spring constants at edges $x=0$, $x=b$, $y=0$ and $y=a$. Similarly, K_{x0}, K_{xb}, K_{y0} and K_{ya} are separately rotational spring constants at corresponding edges. Classical boundary conditions are achieved as below: clamped boundary condition is represented when all the spring constants are set as infinite, when all the spring constants are set as zero the boundary condition is seen as free. Besides, the unit of translational spring and rotational spring constants are separately N/m and N·m/rad.

The transverse displacement of plate is expressed in form of improved Fourier series expansions as below:

$$w(x,y,t)=w(x,y)e^{iwt} \quad (15)$$
$$=\left\{\begin{array}{l}\sum_{m=0}^{\infty}\sum_{n=0}^{\infty}A_{mn}Cos\lambda_m xCos\lambda_n y\\+\sum_{m=0}^{\infty}\sum_{n=1}^{4}B_{mn}Cos\lambda_m xSin\lambda_n y\\+\sum_{m=1}^{4}\sum_{n=0}^{\infty}C_{mn}Sin\lambda_m xCos\lambda_n y\\+\sum_{m=1}^{4}\sum_{n=1}^{4}D_{mn}Sin\lambda_m xSin\lambda_n y\end{array}\right\}e^{iwt}$$

Where A_{mn}, B_{mn}, C_{mn} and D_{mn} are the expansion coefficients, $\lambda_m=m\pi/a$, $\lambda_n=n\pi/b$. $e^{i\omega t}$ is the Harmonic time factor introduced to indicate transverse displacement

at different times. It is easy to find that except for the standard double cosine Fourier series, three supplementary Fourier series are also included in Eq. (15). The governing equation of plate is four-order differential, which recuires the third derivative of transverse displacement admissible function is continuous and the fourth derivative exists at all points in whole solution region. The potential discontinuity associated with the original governing equation is transferred to auxiliary series functions. Then, the Fourier series would be smooth enough in the whole solving domain.

For the sake of neglecting in-plane vibration of plate, strain energy of the plate caused by bending can be expressed as below:

$$V_p = \frac{1}{2}D\int_0^a\int_0^b \begin{bmatrix} \left(\frac{\partial^2 w(x,y,t)}{\partial^2 x}\right)^2 + \left(\frac{\partial^2 w(x,y,t)}{\partial^2 y}\right)^2 \\ +2\mu\left(\frac{\partial^2 w(x,y,t)}{\partial^2 x}\right)\left(\frac{\partial^2 w(x,y,t)}{\partial^2 y}\right) \\ +2(1-\mu)\left(\frac{\partial^2 w(x,y,t)}{\partial x \partial y}\right)^2 \end{bmatrix} \mathrm{d}x\mathrm{d}y \quad (16)$$

Accordingly, the total kinetic energy of the plate and the potential energy stored in springs are separately represented as below:

$$T = \frac{1}{2}\rho h\int_0^a\int_0^b \left(\partial w(x,y,t)/\partial t\right)^2 \mathrm{d}x\mathrm{d}y \quad (17)$$

$$\begin{aligned} V_s &= \frac{1}{2}\int_0^a \left\{ \begin{bmatrix} k_{y0}w(x,y,t)^2 + K_{y0}\left(\frac{\partial w(x,y,t)}{\partial y}\right)^2 \end{bmatrix}_{y=0} \right. \\ &\quad \left. + \begin{bmatrix} k_{yb}w(x,y,t)^2 + K_{yb}\left(\frac{\partial w(x,y,t)}{\partial y}\right)^2 \end{bmatrix}_{y=b} \right\} \mathrm{d}x \\ &\quad + \frac{1}{2}\int_0^b \left\{ \begin{bmatrix} k_{x0}w(x,y,t)^2 + K_{x0}\left(\frac{\partial w(x,y,t)}{\partial x}\right)^2 \end{bmatrix}_{x=0} \right. \\ &\quad \left. + \begin{bmatrix} k_{xa}w(x,y,t)^2 + K_{xa}\left(\frac{\partial w(x,y,t)}{\partial x}\right)^2 \end{bmatrix}_{x=a} \right\} \mathrm{d}y \end{aligned} \quad (18)$$

In the above formulas (16)-(18), ρ means density of rectangular thin plate, h is the thickness of the plate, μ is the Poisson's ratio, and $D = Eh^3/(12(1-\mu^2))$ represents flexural rigidity of the plate.

Power of the external load is expressed as below:

$$W_e = \int_0^a\int_0^b f(x,y)w(x,y)\,\mathrm{d}x\mathrm{d}y \quad (19)$$

$$W_e = \int_0^a\int_0^b F\delta(x-x_e)\,\delta(y-y_e)w(x,y)\,\mathrm{d}x\mathrm{d}y \quad (20)$$

The external load $f(x,y)$ in Eq. (19) is uniform load and external load F in Eq. (20) represents concentrated force, $\delta(x)$ is the Dirac delta function, (x_e, y_e) represents the location of concentrated force.

Lagrangian function of the plate is expressed as below:

$$L = V_p + V_s - T - W_e \quad (21)$$

Substituting Eqs. (16)-(20) into Eq. (21), partial derivatives of Fourier series expansions coefficients are expressed as below:

$$\frac{\partial L}{\partial A_{mn}} = 0 \quad (22)$$

$$\frac{\partial L}{\partial B_{mn}} = 0 \quad (23)$$

$$\frac{\partial L}{\partial C_{mn}} = 0 \quad (24)$$

$$\frac{\partial L}{\partial D_{mn}} = 0 \quad (25)$$

A group of linear algebraic equations about the unknown Fourier coefficients of the displacement function are obtained by Rayleigh–Ritz procedure. They can be summed up in the matrix form:

$$\left(K - \omega^2 M\right)A = F \quad (26)$$

K and M respectively represents stiffness matrix and mass matrix.

2.2 Sound radiation model

Based on the model of rectangular thin plate mentioned before, the sound pressure at arbitrary point in sound field of plate under external load is expressed as below:

$$p(X) = \frac{j\omega\rho_0}{2\pi}\int_S v_n(Y)\frac{e^{-jkr}}{r}dS \quad (27)$$

In Eq. (27), X means field point of sound field, Y is source point, ω is circular frequency of external load, ρ_0 denotes the density of air, c is the sound velocity in air, $k = \omega/c$ means wave number, $r = |X - Y|$ is the distance between point X and Y.

The structure is divided into T finite elements, each discrete element of structure can be seen as point sound source, and Eq. (27) can be described as below:

$$p(X) = \frac{\omega\rho_0}{2\pi}\sum_{i=1}^{T} v_n(Y)\frac{\sin(kr)}{r}\Delta S \quad (28)$$

Where $v_n(Y)$ is the derivation of transverse displacement function, ΔS denotes the area of finite element.

When the surface of the structural radiation coincides with the surface of the observation point, the acoustic radiated power of the plate can be defined as below:

$$W_p = \frac{\omega\rho_0}{4\pi}\int_{S'}\left[\int_S v(Y)\frac{\sin(kr)}{r}v^*(Y_0)dS\right]dS' \tag{29}$$

When the structure is divided into C finite elements, equation (29) can be written as below:

$$W_p \approx \frac{\omega\rho_0}{4\pi}\sum_{i=1}^{C}\sum_{j=1}^{C} v(\vec{r_i})v^*(\vec{r_j})\frac{\sin(kr)}{r}(\Delta S)^2 \tag{30}$$

In the above equation (30), $\vec{r_i}$ means position vector of center point of arbitrary element, r is the distance between center points of arbitrary two elements. The velocity of center of each discrete element can be described in the form column vector namely $v = (v_1, v_2, v_3, \ldots, v_N)^T$, acoustic radiated power is simplified as below:

$$W_p = v^H Z v \tag{31}$$

Where $\boldsymbol{Z}$ is the impedance matrix and H denotes Conjugate transpose, $\boldsymbol{Z}$ can be written in the form as below:

$$Z = \frac{\omega^2\rho_0 S^2}{4\pi N^2 c}\begin{bmatrix} 1 & \frac{\sin(kr_{1,2})}{kr_{1,2}} & \cdots & \frac{\sin(kr_{1,N})}{kr_{1N}} \\ \frac{\sin(kr_{21})}{kr_{21}} & 1 & \cdots & \frac{\sin(kr_{2,N})}{kr_{2,N}} \\ \vdots & \vdots & \ddots & \vdots \\ \frac{\sin(kr_{N,1})}{kr_{N,1}} & \frac{\sin(kr_{N,2})}{kr_{N,2}} & \cdots & 1 \end{bmatrix} \tag{32}$$

Finally, acoustic radiated power level of the rectangular thin plate is expressed as below:

$$L_{W_p} = 10\lg\frac{v^H Z v}{W_0} \tag{33}$$

3 Numerical examples and Discussion

3.1 Convergence and boundary springs study

The series is numerically truncated in actual calculations, and the precision would change with the truncation number. Therefore, it is of significance to verify the effect of truncation number on convergence of current method. In addition, one advantage of current method is that general boundary conditions can be easily achieved by varying stiffness value of springs at each edge. Thus, the effects of the stiffness value of boundary springs on the natural frequencies of thin plate should also be investigated.

Natural frequencies with subject to different truncated configurations are computed to confirm the convergence of the modified Fourier series method for the rectangular thin plate. The geometric and material parameters of the rectangular thin plates are: length of the plate a = 2m, breadth of the plate b=1m and thickness of the plate h = 0.002m, $E = 2.1\times10^{11}$Pa, ρ = 7850Kg/m^3, μ = 0.3. The first six nondimensional frequency parameters $\Omega = \omega a^2(\rho h/D)^{1/2}$ of the simply supported rectangular thin plate with different truncation number M, N are listed in Table 1. To simplify the study, a symbolism is employed in the below research, *e.g.* F, C, S, E respectively denotes the plate with free, clamped, simply supported and elastic boundary condition. In the case of FEM analysis, ABAQUS is employed with 10^5 finite elements. The comparison results in Table 1 prove fast convergence and good accuracy of the current method when truncation number $M = N = 13$. Therefore, the following calculations will be conducted with the truncation number $M = N = 13$.

As discussed in 2.1, general boundary conditions can be simulated by changing the stiffness of springs along each edge. When the stiffness of translational springs and rotational springs are individually set as 10^{10}N/m and 0 N·m/rad, boundary condition can be seen as simply supported. With the stiffness of rotational springs gradually increased, the first three natural frequencies of plate are displayed in Figure 2. It is easy to find that with the increase of stiffness value of rotational springs, the natural frequency of plate grows. Especially in the region between 10^2 and 10^5 N·m/rad, the natural frequency of plate changes rapidly. When the stiffness value of rotational

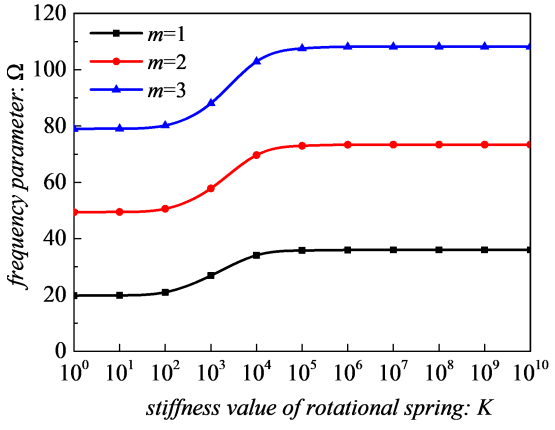

Figure 2: Realtionship between Non-dimensional frequency parameters snd stiffiness of rotational springs

Table 1: Comparison and convergence of the first six frequency parameters Ω for a C-F-F-F rectangular thin plate with different truncation numbers.

$M = N$	Mode number					
	1	2	3	4	5	6
5	3.473	8.512	21.295	27.201	30.973	54.212
6	3.472	8.511	21.293	27.200	30.971	54.205
7	3.472	8.509	21.290	27.200	30.964	54.197
8	3.472	8.508	21.288	27.199	30.963	54.195
9	3.471	8.508	21.288	27.199	30.961	54.193
10	3.471	8.508	21.287	27.199	30.960	54.191
11	3.471	8.507	21.286	27.199	30.959	54.190
12	3.471	8.507	21.286	27.199	30.958	54.189
13	3.471	8.507	21.286	27.199	30.957	54.188
14	3.471	8.507	21.285	27.199	30.957	54.187
FEM	3.470	8.506	21.285	27.198	30.956	54.187
Li *et al.* [27]	3.470	8.505	21.281	27.201	30.955	54.185

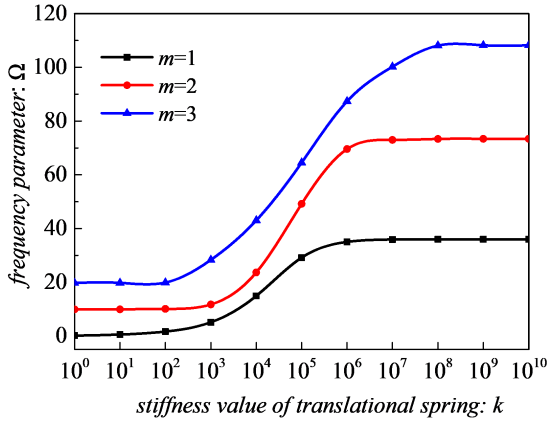

Figure 3: Realtionship between Non-dimensional frequency parameters snd stiffiness of translational springs

spring is greater than 10^{10} N·m/rad, the natural frequency of plate is almost invariant. Which means the boundary condition has changed from simply supported to clamped.

When the stiffness of rotational springs are set as 10^{10} N·m/rad, the first three natural frequencies of plate with different translational springs stiffness are displayed in Figure 3. It can be concluded from Figure 3 that the natural frequency of plate varies fiercely when the stiffness of translational springs are ranged from 10^2 N/m to 10^7 N/m. The natural frequency of plate is almost invariant when the stiffness value of translational spring is bigger than 10^{10} N/m. In summary, when the stiffness of rotational springs and translational springs are individually set as 10^{10} N·m/rad and 10^{10}N/m, it can be seen as clamped boundary condition in the current method. From the comparison between Figure 2 and Figure 3, it is easy to find the stiffness value of translational springs has greater effect on natural frequency than rotational springs. In the following discussion, the corresponding spring stiffness values for general boundary conditions are given in Table 2. For the sake of simplicity, a four-letter string is employed to represent the restraint condition of a plate. For example, C-F-C-S stands for the plate with edges $x = 0$, $x = b$, $y = 0$, $y = a$ having clamped, free, clamped and simply-supported boundary conditions respectively.

Table 2: Stiffness value of springs on each edge for different boundary conditions.

Boundary condition	k(N/m)	K (N·m/rad)
F	0	0
C	10^{10}	10^{10}
S	10^{10}	0
E	10^5	10^{10}

3.2 Free vibration analysis

The nondimensional natural frequency parameters $\Omega = \omega a^2(\rho h/D)^{1/2}$ obtained by current method are in comparison with the results of related literature [48] and ABAQUS in this section. The plate in this subsection is of same material property with example in 3.1. Tables 3-5 illustrate the comparison of Ω with different boundary conditions. The tiny distinction verifies the accuracy of current method. The first six mode shapes of clamped plate using current

Table 3: Comparison of the first six frequency parameters Ω for the rectangular thin plate with C-F-F-F boundary condition.

$r = a/b$	Source	Mode number					
		1	2	3	4	5	6
1	Present	3.468	8.506	21.295	27.289	30.866	54.167
	Li *et al.* [27]	3.470	8.505	21.281	27.201	30.955	54.185
	ABAQUS	3.471	8.488	21.258	27.190	30.866	54.105
1.5	Present	3.451	11.657	21.465	39.363	53.541	61.615
	ABAQUS	3.453	11.654	21.462	39.319	53.544	61.606
2.0	Present	3.429	14.812	21.454	48.188	60.249	92.510
	ABAQUS	3.439	14.810	21.453	48.181	60.199	92.507

Table 4: Comparison of the first six frequency parameters Ω for the rectangular thin plate with C-C-C-C boundary condition.

$r = a/b$	Source	Mode number					
		1	2	3	4	5	6
1	Present	35.975	73.391	73.392	108.20	131.57	131.19
	Li *et al.* [27]	35.985	73.393	73.393	108.21	131.58	132.20
	ABAQUS	35.970	73.355	73.355	108.05	131.37	132.08
1.5	Present	60.759	93.831	148.50	149.67	179.26	226.82
	ABAQUS	60.753	93.720	148.57	149.57	179.17	226.73
2.0	Present	98.308	127.28	179.05	253.02	255.81	284.25
	ABAQUS	98.312	126.99	178.95	252.96	255.60	283.50

Table 5: Comparison of the first six frequency parameters Ω for the rectangular thin plate with S-S-S-S boundary condition.

$r = a/b$	Source	Mode number					
		1	2	3	4	5	6
1	Present	21.670	51.301	51.301	80.917	100.661	100.662
	Li *et al.* [27]	21.500	51.187	51.187	80.816	100.58	100.59
	ABAQUS	21.600	51.200	51.200	80.820	100.600	100.601
1.5	Present	33.937	63.350	100.766	112.607	130.235	179.454
	ABAQUS	34.002	63.660	100.771	112.701	129.995	179.531
2.0	Present	52.650	81.755	130.777	171.477	199.683	200.826
	ABAQUS	52.700	81.802	130.801	170.480	200.001	200.101

method and ABAQUS are respectively plotted in Figure 4. It is helpful to understand certain features in the vibration characteristics of rectangular plate.

Based on the validation of accuracy of current method, the effect of dimensional parameters and elastic boundary condition on frequency of plate is discussed. The first six natural frequencies of thin plate with different aspect ratios and boundary conditions are shown in Table 6 and Table 7. Meanwhile, the relations between first three natural frequencies and aspect ratios are shown in Figure 5 and Figure 6. It's easy to find that with the increase of aspect ratios, the natural frequency increases. When the aspect ratio is greater than 10, the natural frequency is almost invariant.

In the above analysis, boundary conditions are limited to classical boundary conditions. However, elastic boundary conditions are more commonly encountered in practical engineering. Table 8 and Table 9 show the first six frequency parameters of thin plate with edges elastically restrained such as C-C-C-E, S-S-E-E and F-F-E-E. What is interesting about the data in Table 8 and Table 9 is that in the combination of clamped boundary condition and elastic boundary condition, with the increase region of clamped boundary condition the frequency parameter $\Omega = \omega a^2(\rho h/D)^{1/2}$ increases. Meanwhile, in the combination

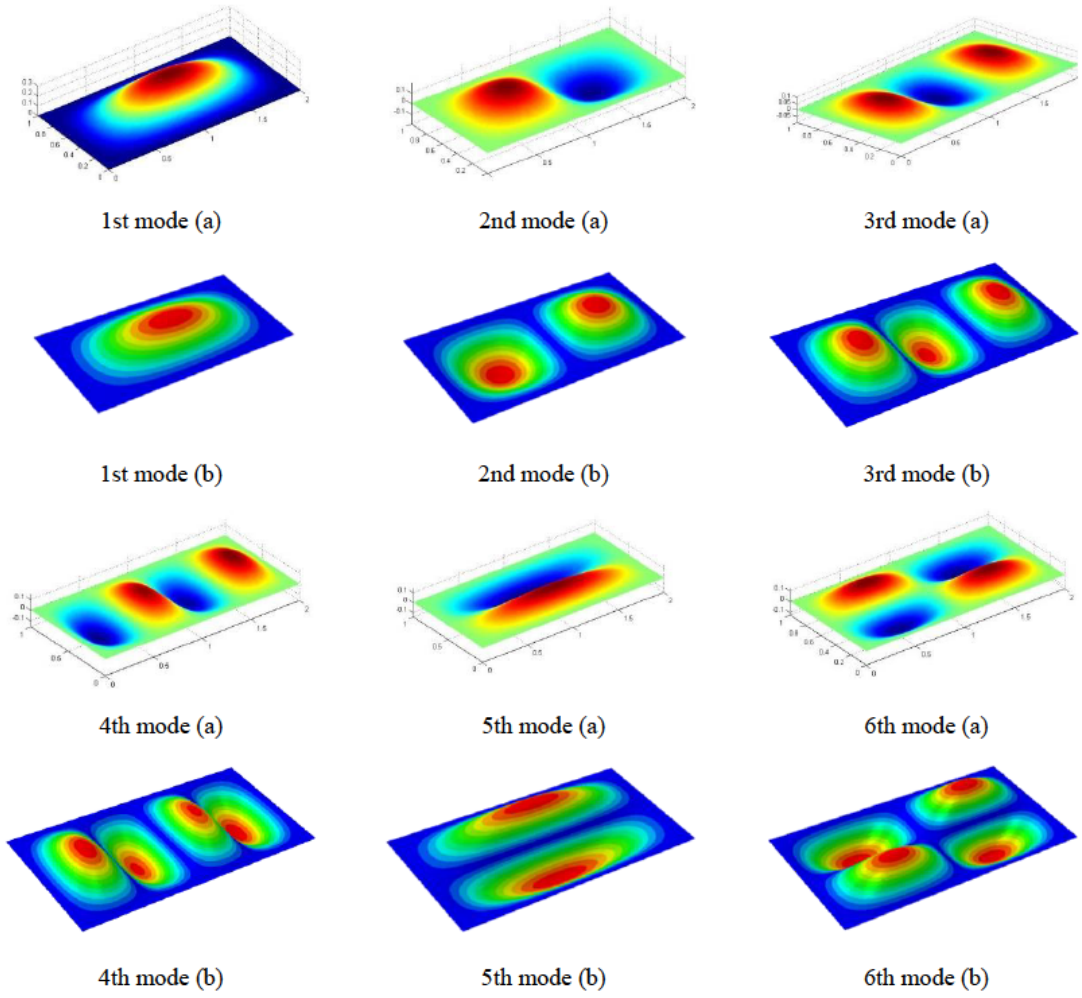

Figure 4: The first six mode shapes of rectangular thin plate with C-C-C-C boundary condition: (a) Current method (b) Abaqus

Table 6: The first six natural frequencies for the rectangular thin plate with S-S-S-S boundary condition and different aspect ratios.

$r = a/b$	Mode number					
	1	2	3	4	5	6
1	9.771	24.428	24.428	39.085	48.856	48.857
1.5	7.057	13.571	21.714	24.428	28.228	39.085
2	6.107	9.771	15.878	20.764	24.428	24.428
2.5	5.667	8.012	11.921	17.393	20.324	22.669
3	5.429	7.057	9.771	13.571	18.457	20.086
4	5.191	6.107	7.634	9.771	12.520	15.878
5	5.081	5.667	6.645	8.013	9.771	11.921
6	5.021	5.429	6.107	7.057	8.279	9.771
7	4.985	5.285	5.783	6.481	7.378	8.475
8	4.962	5.191	5.573	6.107	6.794	7.634
9	4.946	5.127	5.429	5.851	6.394	7.057
10	4.935	5.081	5.325	5.667	6.107	6.645
11	4.926	5.047	5.249	5.532	5.895	6.339

Table 7: The first six natural frequencies for the rectangular thin plate with C-C-F-F boundary condition and different aspect ratios.

$r = a/b$	Mode number					
	1	2	3	4	5	6
1	10.974	13.073	21.582	30.285	33.255	39.511
1.5	4.861	6.773	13.414	15.592	16.257	25.981
2	2.727	4.449	7.524	10.192	13.544	14.782
2.5	1.741	3.292	4.801	7.290	9.436	12.431
3	1.207	2.610	3.326	5.641	6.537	9.388
4	0.676	1.845	1.864	3.662	3.872	6.070
5	0.432	1.190	1.428	2.336	2.949	3.872
6	0.299	0.824	1.165	1.618	2.384	2.681
7	0.219	0.605	0.984	1.186	1.965	2.002
8	0.168	0.462	0.852	0.907	1.502	1.727
9	0.132	0.365	0.716	0.751	1.185	1.519
10	0.107	0.295	0.579	0.672	0.958	1.356
11	0.088	0.244	0.478	0.608	0.791	1.184

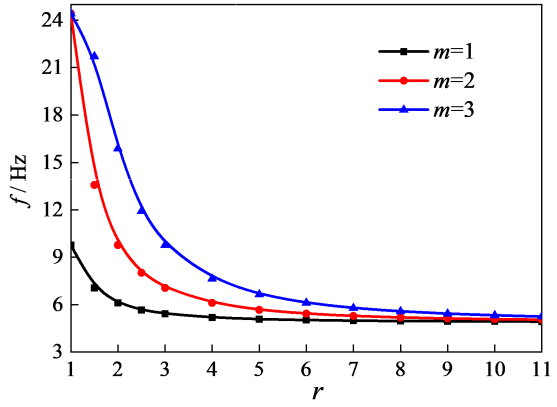

Figure 5: Realtionship between natural frequencies snd aspect ratio with S-S-S-S boundary condition

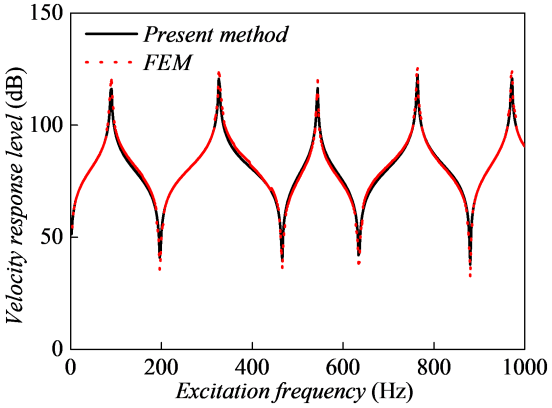

Figure 7: The velocity response of point (0.5,0.5) with C-C-C-C boundary condition

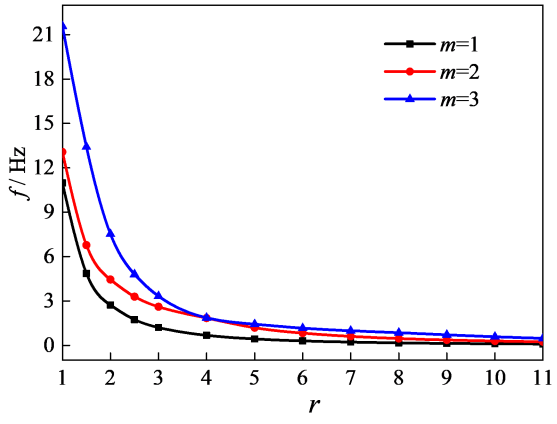

Figure 6: Relationship between natural frequencies snd aspect ratio with C-C-F-F boundary condition

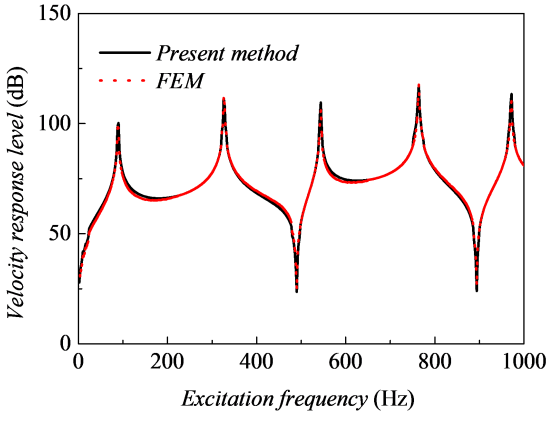

Figure 8: The velocity response of point (0.2,0.3) with C-C-C-C boundary condition

Table 8: The first six parameters Ω for the rectangular thin plates with elastic boundary conditions and different aspect ratios.

Ratio r	Mode number	Boundary condition				
		C-C-C-E	C-C-E-E	C-E-E-E	E-E-E-E	S-S-S-E
1	1	33.754	32.189	30.457	29.169	22.182
	2	59.263	52.225	50.417	49.192	48.237
	3	69.747	67.685	55.333	49.196	48.604
	4	91.678	77.000	70.605	64.532	71.725
	5	96.489	83.143	74.259	70.903	82.664
	6	127.065	108.362	90.447	74.599	95.727
1.5	1	56.414	53.159	52.536	51.983	40.135
	2	87.378	83.081	78.901	75.676	64.589
	3	118.712	103.699	102.989	102.397	100.224
	4	141.000	127.412	119.885	110.025	109.360
	5	144.928	135.956	122.755	119.418	121.115
	6	193.532	159.885	156.656	146.593	161.383
2	1	91.254	85.866	85.533	85.243	65.662
	2	117.624	110.700	108.748	107.026	88.729
	3	166.273	157.983	150.609	145.346	131.272
	4	204.100	178.161	177.750	177.380	173.281
	5	226.553	197.675	195.366	193.435	192.948
	6	237.579	228.259	208.456	194.921	194.418
2.5	1	137.334	129.299	129.079	128.899	98.630
	2	160.418	150.510	149.353	148.317	120.781
	3	204.113	192.221	188.439	185.107	161.421
	4	270.414	256.904	246.754	238.450	222.255
	5	314.536	274.658	274.361	274.119	267.284
	6	335.077	291.831	290.393	289.136	286.327
3	1	194.204	182.963	182.807	182.686	138.997
	2	215.099	201.769	201.019	200.286	160.528
	3	254.715	238.789	236.491	234.081	199.643
	4	315.980	297.729	291.730	286.417	258.357
	5	400.076	379.768	366.959	354.642	337.543
	6	449.806	392.928	392.731	392.503	382.252
3.5	1	252.189	246.701	246.619	246.488	186.706
	2	274.489	263.862	263.312	262.773	207.851
	3	281.078	297.287	295.624	294.112	245.763
	4	351.198	350.970	347.072	343.349	302.608
	5	374.110	427.171	418.886	411.329	379.555
	6	502.399	526.706	510.274	495.878	477.109

of simply supported, free and elastic boundary condition, with the increase region of elastic boundary condition the frequency parameter $\Omega = \omega a^2(\rho h/D)^{1/2}$ magnifies.

3.3 Forced vibration analysis

The validity of current method to the forced vibration of clamped thin plate is discussed in this subsection. Point force is considered as the exciting force, the magnitude is 100N. The location of point force is the center of rectangular thin plate. The plate is of same material property with the plate in 3.1. The geometric parameters are as below: length a = 1m, breadth b = 1m and thickness h = 0.01m. The points of A (0.5, 0.5) and B (0.2, 0.3) on the plate are chosen as the examination point. Figure 7 and Figure 8 respectively displays velocity response of point A and B. The result of current method matches well with the result of

Table 9: The first six parameters Ω for the rectangular thin plates with elastic boundary conditions and different aspect ratios.

Ratio r	Mode number	Boundary condition				
		S-S-E-E	S-E-E-E	F-F-F-E	F-F-E-E	F-E-E-E
1	1	24.714	26.756	8.185	19.543	20.739
	2	47.561	48.358	8.445	22.173	31.896
	3	48.009	48.744	18.951	35.136	43.958
	4	67.199	65.540	27.870	42.926	53.154
	5	73.373	72.933	28.068	45.910	55.835
	6	93.924	80.178	46.199	58.428	68.620
1.5	1	48.657	50.071	7.747	44.089	45.157
	2	67.421	71.599	14.065	46.932	55.341
	3	101.073	101.686	31.414	58.620	80.831
	4	108.026	109.200	45.889	86.975	97.697
	5	116.744	118.136	53.863	96.713	106.549
	6	151.198	148.488	68.458	99.770	120.851
2	1	82.884	83.894	21.082	78.486	79.494
	2	98.861	102.698	42.939	81.366	88.955
	3	134.042	139.900	63.969	92.678	112.250
	4	176.394	176.849	73.902	117.583	153.333
	5	190.238	191.812	91.444	162.818	173.005
	6	192.035	193.679	113.479	172.061	181.525
2.5	1	127.117	127.891	29.437	122.742	123.682
	2	141.459	144.624	47.347	125.594	132.683
	3	172.362	178.588	83.824	136.761	154.017
	4	224.676	231.849	111.930	159.639	192.428
	5	273.338	273.708	136.638	200.164	249.590
	6	286.278	287.633	147.401	262.685	269.892
3	1	181.266	181.895	9.283	176.935	177.581
	2	194.628	197.233	39.298	179.648	186.375
	3	222.427	228.080	60.702	191.268	205.987
	4	269.682	278.076	95.207	212.410	241.457
	5	339.301	347.347	158.304	251.670	296.225
	6	391.881	392.188	191.591	306.672	369.081
3.5	1	245.340	245.835	50.661	240.835	241.725
	2	258.040	260.229	74.098	243.526	250.244
	3	283.652	288.590	108.545	254.648	268.965
	4	326.761	334.866	149.489	275.451	302.147
	5	390.935	401.180	232.355	310.261	353.029
	6	477.963	487.258	247.703	362.905	423.776

FEA, which validates the effectiveness of present method to the forced vibration.

3.4 Acoustic radiation characteristics analysis

The effect of boundary condition and location of point force on acoustic radiation characteristics are discussed in this section. The tiny distinction displayed in Figure 9 and Figure 10 verifies the accuracy of current method when analyzing acoustic radiation characteristics of plate.

Monitoring point is located 0.1m above the center of the plate. Figure 11-12 individually provides the comparison of sound pressure level and sound power level with different boundary edges. It is apparent from Figure 11-12 that both sound pressure level and sound power level reach the peak when the frequency of excitation force equals first or-

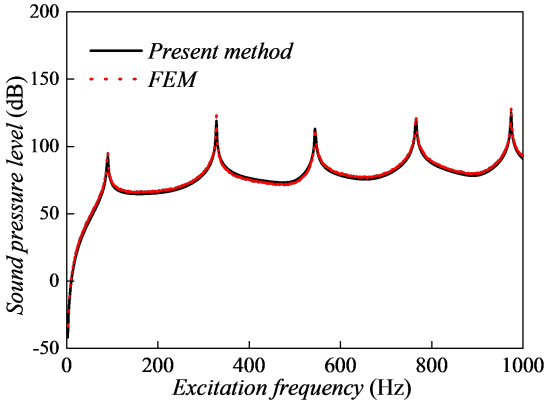

Figure 9: The comparison of sound pressure level with C-C-C-C boundary

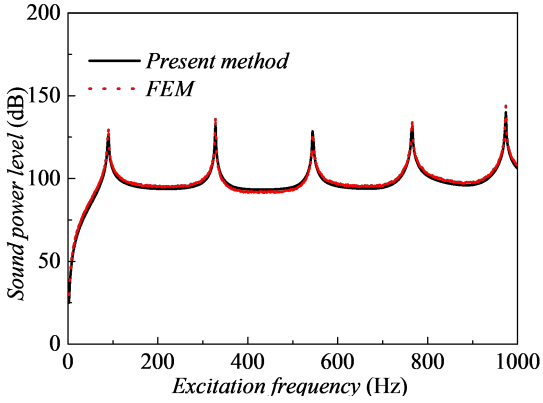

Figure 10: The comparison of sound poewr level with C-C-C-C boundary condition

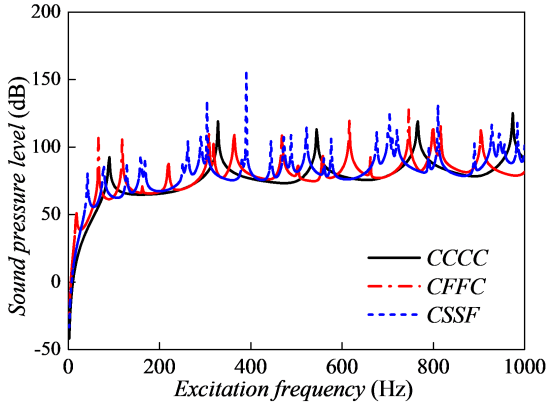

Figure 11: Sound pressure level with different boundary conditions

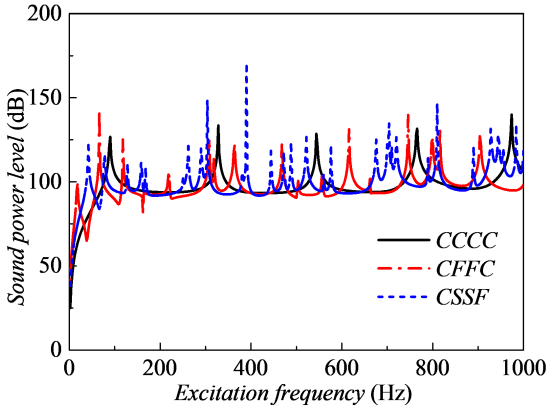

Figure 12: Sound power level with different boundary conditions

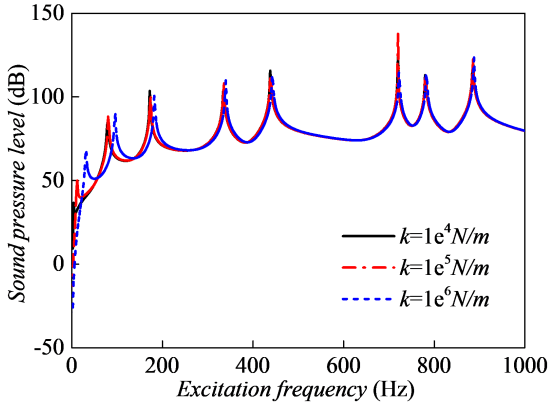

Figure 13: Sound pressure level with different elastic boundary conditions

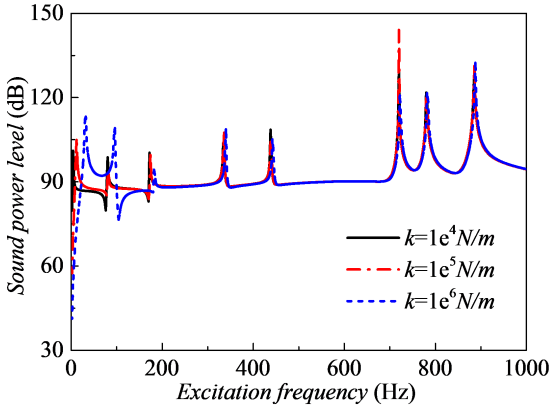

Figure 14: Sound power level with different elastic boundary conditions

der natural frequency of plate. Meanwhile, with the weakening of boundary condition more peaks appear and the maximum peak value becomes bigger.

Figure 13 and Figure 14 individually presents the comparison of sound pressure level and sound power level of plate when the stiffness value of translational springs k are different. From the Figure 13 and Figure 14, it can be seen that with the increase of stiffness value of translational spring, the peak value varies and exists at different loca-

tion beyond 400Hz. However, the peak value is almost invariant when the frequency is greater than 400Hz.

Figure 15 and Figure 16 individually compares the sound pressure and sound power of clamped plate when the location of point force is different. From the data in Figure 15 and Figure 16, we can see that the first peak value exists at same location of horizontal axis. In addition, with the point force moving to the center of plate, the number of peak decreases, whereas the peak value increases.

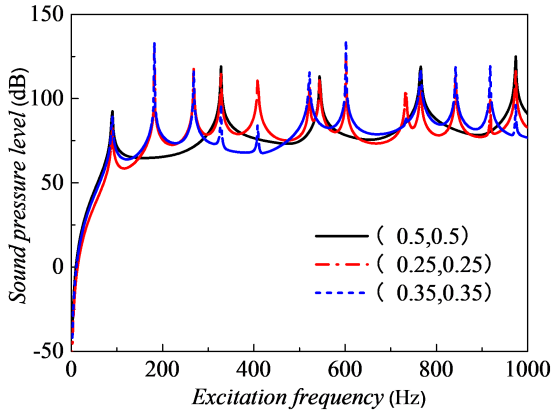

Figure 15: Sound pressure level of plate with different location of point force

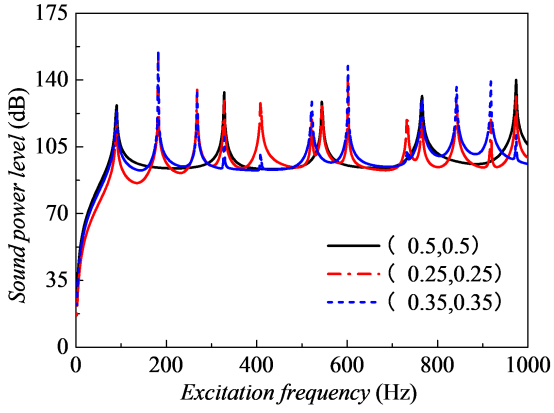

Figure 16: Sound power level of plate with different location of point force

4 Conclusions

This paper describes a unified Improved Fourier Series Method (IFSM) for the vibration and acoustic characteristics analysis of rectangular thin plates with general boundary conditions. Sine function term is introduced to modify the discontinuity of traditional Fourier Series Method on boundary. The unknown coefficients are solved by using the Rayleigh–Ritz procedure. General boundary conditions can be easily achieved by varying stiffness value of springs on each edge. The method in this paper is of fast convergence and good accuracy by comparing with the result of related literature and FEM. With the application of the present method, there is no need to reformulate the mass and stiffness matrices of the plate for the analysis on the vibration and sound radiation characteristic of plate with different boundary edges.

The study has identified the stiffness values of translational springs have greater effect on natural frequency of plate than rotational springs. With the increase of aspect ratios, the natural frequency increases. Natural frequency of thin plate varies greatly with different boundary conditions. In the combination of clamped boundary condition and elastic boundary condition, with the increase region of clamped boundary condition the frequency parameter increases.

The research has also shown that sound pressure level and sound power level of plate reach the peak value when the frequency of excitation force equals first order natural frequency of plate. Meanwhile, with the weakening of boundary condition more peaks appear and the maximum peak value becomes bigger. When the point force moves to the center of four edges clamped plate, the number of peak decreases, whereas the peak value increases.

Funding: This study was funded by National key Research and Development program(2016YFC0303406), Fundamental Research Funds for the Central University(HEUCFM170113), High Technology Ship Funds of Ministry of Industry and Information of P.R. China, Assembly Advanced Research Fund Of China (6140210020105), National Natural Science Foundation of China (51209052), China Postdoctoral Science Foundation(2014M552661), Major innovation projects Of High Technology Ship Funds of Ministry of Industry and Information of P.R.China, Naval pre-research project.

Conflict of Interests: The authors declare that they have no conflict of interest.

Data Availability Statement: The data used to support the findings of this study are included within the article.

References

[1] Liew, K.M., K.Y. Lam, and S.T. Chow, Free vibration analysis of rectangular plates using orthogonal plate function. Computers & Structures, 1990. 34(1): p. 79-85.

[2] Wu, J.H., A.Q. Liu, and H.L. Chen, Exact Solutions for Free-Vibration Analysis of Rectangular Plates Using Bessel Functions. Journal of Applied Mechanics, 2007(6).

[3] Takashi, M. and Y. Jin, Application of the collocation method to vibration analysis of rectangular mindlin plates. Computers & Structures, 1984. 18(3): p. 425-431.

[4] Liew, K.M. and T.M. Teo, THREE-DIMENSIONAL VIBRATION ANALYSIS OF RECTANGULAR PLATES BASED ON DIFFERENTIAL QUADRATURE METHOD. Journal of Sound and Vibration, 1999. 220(4): p. 577-599.

[5] Liu, G.R. and X.L. Chen, A MESH-FREE METHOD FOR STATIC AND FREE VIBRATION ANALYSES OF THIN PLATES OF COMPLICATED SHAPE. Journal of Sound and Vibration, 2001. 241(5): p. 839-855.

[6] Bert, C.W., S.K. Jang, and A.G. Striz, Two new approximate methods for analyzing free vibration of structural components. Aiaa Journal, 2015. 26(5): p. 612-618.

[7] Wanji, C. and Y.K. Cheung, Refined triangular discrete Kirchhoff plate element for thin plate bending, vibration and buckling analysis. International Journal for Numerical Methods in Engineering, 1998. 41(8): p. 1507-1525.

[8] Lim, C.W., et al., On new symplectic elasticity approach for exact free vibration solutions of rectangular Kirchhoff plates. International Journal of Engineering Science, 2009. 47(1): p. 131-140.

[9] Li, S. and H. Yuan, Green quasifunction method for free vibration of clamped thin plates. Acta Mechanica Solida Sinica, 2012. 25(1): p. 37-45.

[10] Tornabene, F., 2-D GDQ solution for free vibrations of anisotropic doubly-curved shells and panels of revolution. Composite Structures, 2011. 93(7): p. 1854-1876.

[11] Tornabene, F., N. Fantuzzi, and M. Bacciocchi, Free vibrations of free-form doubly-curved shells made of functionally graded materials using higher-order equivalent single layer theories. Composites Part B Engineering, 2014. 67(1): p. 490-509.

[12] Tornabene, F., et al., Radial basis function method applied to doubly-curved laminated composite shells and panels with a General Higher-order Equivalent Single Layer formulation. Composites Part B Engineering, 2013. 55(1): p. 642-659.

[13] Tornabene, F. and E. Viola, 2-D solution for free vibrations of parabolic shells using generalized differential quadrature method. European Journal of Mechanics - A/Solids, 2008. 27(6): p. 1001-1025.

[14] Tornabene, F. and E. Viola, Free vibration analysis of functionally graded panels and shells of revolution. Meccanica, 2009. 44(3): p. 255-281.

[15] Kang, S.W. and S.N. Atluri, Improved non-dimensional dynamic influence function method for vibration analysis of arbitrarily shaped plates with clamped edges. Advances in Mechanical Engineering, 2016. 8(3).

[16] Li, X.K., J.F. Zhang, and Y. Zheng, Static and Free Vibration Analysis of Laminated Composite Plates Using Isogeometric Approach Based on the Third Order Shear Deformation Theory. Advances in Mechanical Engineering, 2014.

[17] Thai, H.T. and D.H. Choi, A simple first-order shear deformation theory for the bending and free vibration analysis of functionally graded plates. Composite Structures, 2013. 101(15): p. 332-340.

[18] Thai, H.T., T. Park, and D.H. Choi, An efficient shear deformation theory for vibration of functionally graded plates. Archive of Applied Mechanics, 2013. 83(1): p. 137-149.

[19] Thai, H.T. and D.H. Choi, Analytical solutions of refined plate theory for bending, buckling and vibration analyses of thick plates. Applied Mathematical Modelling, 2013. 37(18-19): p. 8310-8323.

[20] Thai, H.T., M. Park, and D.H. Choi, A simple refined theory for bending, buckling, and vibration of thick plates resting on elastic foundation. International Journal of Mechanical Sciences, 2013. 73(73): p. 40-52.

[21] Thai, H.T. and S.E. Kim, Free vibration of laminated composite plates using two variable refined plate theory. International Journal of Mechanical Sciences, 2010. 52(4): p. 626-633.

[22] Dozio, L. and M. Ricciardi, Free vibration analysis of ribbed plates by a combined analytical–numerical method. Journal of Sound & Vibration, 2009. 319(1): p. 681-697.

[23] Dozio, L., On the use of the Trigonometric Ritz method for general vibration analysis of rectangular Kirchhoff plates. Thin-Walled Structures, 2011. 49(1): p. 129-144.

[24] Dozio, L., Natural frequencies of sandwich plates with FGM core via variable-kinematic 2-D Ritz models. Composite Structures, 2013. 96: p. 561-568.

[25] Jayasinghe, S. and S.M. Hashemi, A Dynamic Coefficient Matrix Method for the Free Vibration of Thin Rectangular Isotropic Plates. Shock and Vibration, 2018.

[26] Li, H.C., et al., An Accurate Solution Method for the Static and Vibration Analysis of Functionally Graded Reissner-Mindlin Rectangular Plate with General Boundary Conditions. Shock and Vibration, 2018: p. 21.

[27] Shi, S.X., et al., Modeling and Simulation of Transverse Free Vibration Analysis of a Rectangular Plate with Cutouts Using Energy Principles. Shock and Vibration, 2018: p. 16.

[28] Allahverdizadeh, A., M.H. Naei, and M.N. Bahrami, Nonlinear free and forced vibration analysis of thin circular functionally graded plates. Journal of Sound & Vibration, 2008. 310(4): p. 966-984.

[29] Han, W. and M. Petyt, Linear vibration analysis of laminated rectangular plates using the hierarchical finite element method—II. Forced vibration analysis. Computers & Structures, 1996. 61(4): p. 713-724.

[30] Akay, A., M. Tokunaga, and M. Latcha, A theoretical analysis of transient sound radiation from a clamped circular plate. American Society of Mechanical Engineers, 1984. 51(1): p. 41-47.

[31] Srinivas, S. and A.K. Rao, Bending, vibration and buckling of simply supported thick orthotropic rectangular plates and laminates. International Journal of Solids & Structures, 1970. 6(11): p. 1463-1481.

[32] Shi, D.Y., et al., Free and Forced Vibration of the Moderately Thick Laminated Composite Rectangular Plate on Various Elastic Winkler and Pasternak Foundations. Shock and Vibration, 2017: p. 23.

[33] Inalpolat, M., M. Caliskan, and R. Singh, Analysis of near field sound radiation from a resonant unbaffled plate using simplified analytical models. Noise Control Engineering Journal, 2010. 58(2): p. 145-156.

[34] Mace, B.R., Sound radiation from a plate reinforced by two sets of parallel stiffeners. Journal of Sound and Vibration, 1980. 71(3): p. 435-441.

[35] Laulagnet, B., Sound radiation by a simply supported unbaffled plate. Journal of the Acoustical Society of America, 1998. 103(5):

p. 2451-2462.
[36] Sorokin, S.V., Vibrations of and sound radiation from sandwich plates in heavy fluid loading conditions. Composite Structures, 2000. 48(4): p. 219-230.
[37] Li, H., et al., Vibration analysis of functionally graded porous cylindrical shell with arbitrary boundary restraints by using a semi analytical method. Composites Part B: Engineering, 2019. 164: p. 249-264.
[38] Pang, F., et al., A modified Fourier solution for vibration analysis of moderately thick laminated annular sector plates with general boundary conditions, internal radial line and circumferential arc supports. Curved and Layered Structures, 2017. 4(1): p. 189-220.
[39] Li, H., F. Pang, and H. Chen, A semi-analytical approach to analyze vibration characteristics of uniform and stepped annular-spherical shells with general boundary conditions. European Journal of Mechanics - A/Solids, 2019. 74: p. 48-65.
[40] Pang, F., et al., Application of flügge thin shell theory to the solution of free vibration behaviors for spherical-cylindrical-spherical shell: A unified formulation. European Journal of Mechanics - A/Solids, 2019. 74: p. 381-393.
[41] Li, H., et al., Free vibration analysis of uniform and stepped combined paraboloidal, cylindrical and spherical shells with arbitrary boundary conditions. International Journal of Mechanical Sciences, 2018. 145: p. 64-82.
[42] Li, H., et al., A semi analytical method for free vibration analysis of composite laminated cylindrical and spherical shells with complex boundary conditions. Thin-Walled Structures, 2019. 136: p. 200-220.
[43] Li, H., et al., Application of first-order shear deformation theory for the vibration analysis of functionally graded doubly-curved shells of revolution. Composite Structures, 2019. 212: p. 22-42.
[44] Li, H., et al., Jacobi–Ritz method for free vibration analysis of uniform and stepped circular cylindrical shells with arbitrary boundary conditions: A unified formulation. Computers & Mathematics with Applications, 2018.
[45] Pang, F., et al., Free vibration of functionally graded carbon nanotube reinforced composite annular sector plate with general boundary supports. Curved and Layered Structures, 2018. 5(1): p. 49-67.
[46] Pang, F., et al., Application of First-Order Shear Deformation Theory on Vibration Analysis of Stepped Functionally Graded Paraboloidal Shell with General Edge Constraints. Materials, 2018. 12(1): p. 69.
[47] Pang, F., et al., Free vibration analysis of combined composite laminated cylindrical and spherical shells with arbitrary boundary conditions. Mechanics of Advanced Materials and Structures, 2019: p. 1-18.
[48] Li, W.L., et al., An exact series solution for the transverse vibration of rectangular plates with general elastic boundary supports. Journal of Sound & Vibration, 2009. 321(1): p. 254-269.
[49] Li, H., et al., Free vibration analysis for composite laminated doubly-curved shells of revolution by a semi analytical method. Composite Structures, 2018. 201: p. 86-111.
[50] Pang, F., et al., A semi analytical method for the free vibration of doubly-curved shells of revolution. Computers & Mathematics with Applications, 2018. 75(9): p. 3249-3268.
[51] Pang, F., et al., Free and Forced Vibration Analysis of Airtight Cylindrical Vessels with Doubly Curved Shells of Revolution by Using Jacobi-Ritz Method. Shock and Vibration, 2017. 2017.
[52] Li, H., et al., A semi-analytical method for vibration analysis of stepped doubly-curved shells of revolution with arbitrary boundary conditions. Thin-Walled Structures, 2018. 129: p. 125-144.